

Obtaining the Fracture Resistance Curve Using the General Displacement

Goksel SARACOGLU

Faculty of Aeronautics and Astronautics, Iskenderun Technical University, Iskenderun Hatay, Türkiye,

E-mail: goksel.saracoglu@iste.edu.tr

crossref <http://dx.doi.org/10.5755/j02.mech.31368>

1. Introduction

In laminated composite materials, cracks show branching properties under the influence of stress, depending on fibre orientation and load direction. Each unit progression of these micro-cracks trying to propagate at the fibre-matrix interface has a corresponding material stiffness.

In anisotropic materials, the direction of crack propagation varies depending on the strength of the material and the applied stress [1]. The strength of composite materials varies depending on the size, distribution, specimen shape and size of the defect [2]. The modulus of elasticity, which varies from place to place due to the different content of components and voids, causes the crack propagation force to change moment by moment [3]. Therefore, the fracture toughness of such materials characterizes the resistance to cracking [4].

Branched crack formation at the crack tip continues its planar progression with increasing stress and brings along fibre breaks. The value of fracture toughness against each unit of crack propagation forms the resistance curve (*R*-curve). Fracture toughness creates a balance against the stress intensity factor that tries to propagate the crack. However, at the end of the critical crack length, the equilibrium is upset in favour of the stress intensity factor. This point is called the critical fracture toughness.

Although these details about the *R*-curve are known, constructing the curve is a complex process. Currently, the most widely used method is the compliance matching to utilize the graph of the load versus the crack mouth opening displacement (*P*-CMOD). However, the absence of an equation to make the measurements continuous causes the *R*-curve to be formed with the data taken from certain points.

In the compliance matching method, the compliance of each crack length to width ratio a/W of the material whose resistance curve is to be extracted is determined and the compliance curve is created. In the *P*-CMOD curve, the compliances formed by the lines drawn at some points from the origin to the various (and maximum) load are determined and the amount of crack propagation Δa measured by taking the general compliance of the material as a guide [5].

Accurate estimation of crack length a/W using applied load P and CMOD or crack propagation data recorded during the test is critical in the evaluation of *R*-curves. The most accurate result is to measure the amount of crack propagation. However, tracking this propagation is more difficult than measuring CMOD. In a study, an empirical formulation between CMOD and crack propagation amount was developed and crack propagation was determined from CMOD measurement [6].

Finite Fracture Mechanics models, used for the preliminary design and optimization of composite structures and using laminate thickness as a representative length scale, have been developed to predict the fracture of multi-directional composite laminates in the presence of stress concentrations [7-9]. It is based on the simultaneous fulfilment of an energy-based criterion requiring fracture toughness [7-9] or crack resistance curve [10].

The recently used Size Effect Law method is based on the idea that brittle materials of different sizes cannot have the same strength. According to the model, as the specimen size increases, the strength and fracture toughness will increase. Since the fracture toughness value in the crack resistance curve is the tangent of the *G*-curve and the *R*-curve, the *G*-curve, which varies with specimen size, will form the *R*-curve, which is independent of specimen size [11]. This method was later inspired for mode-I dynamic conditions and the *R*-curve for dynamic environment was determined by preparing the same specimen type but with different dimensions [12]. These studies have also yielded important results in terms of indicating that the fracture toughness of polymeric composite material subjected to dynamic stress is 63% higher than the static fracture toughness.

The studies carried out in the creation of *R*-curves were mostly on random-short fibre reinforced composite materials [5, 13-14]. Considering the determination of the critical fracture stress next to the resistance curve, the concept of crack tip opening displacement (CTOD) was introduced [14]. The compliance-matching method was generally accepted and started to be applied to graphite-epoxy laminate composites [15]. Then, the resistance curve based on energy absorption related to the micro-mechanism of fracture was constructed and the curve slope and cut-off points were standardized according to the composite structures [16-17].

In experimental fracture mechanics, strain-gage based techniques for the determination of stress intensity factors are quite popular due to their ease of operation, cost effectiveness and ability to measure strains in the high strain gradient zones compared to other methods such as photoelasticity [18], caustics [19-20] and DIC (Digital Image Correlation) [21].

In compliance-matching method, the comparison of the behaviour of damaged and fresh specimens was carried out in a study [22]. In this study, it was noted that the *P*-COD curve and fracture load of the damaged specimen differed from that of a fresh specimen with a machined crack of length equal to the estimated crack length in the damaged specimen.

When the studies are examined, it is seen that the fracture energy-crack propagation graph is not obtained by

using all the data of the load-displacement curve. It was mostly created by using the data obtained from fresh specimens with different crack lengths. The R -curve that will be formed from the values of specimens with different crack lengths but artificially brought to this crack level will not reflect the actual situation. In this study, the equations for the complete transformation of the load-displacement curve of a specimen were generated and Linear Elastic Fracture Mechanics and energy methods were utilised in this context. Therefore, a method suitable for specimens with linear characteristics has been developed. For this, a laminated composite tensile specimen with a single edge crack in $[0/90]_{4s}$ glass fibre/epoxy structure was used.

2. The proposed method

In the proposed methodology, the extensometer is attached to the single side-cracked tensile specimen. The specimen length measured with the extensometer is approximately $2W$ (W specimen width). Measuring the effect of crack propagation on extensometer length stiffness is the main idea of the proposed methodology.

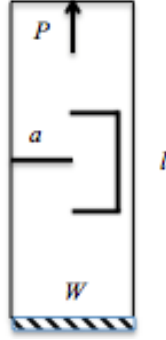


Fig. 1 Schematic view of single-sided crack tensile specimen with extensometer

The relationship between the stiffness k and the displacement Δl of the part under the load ΔP is as in Eq. (1):

$$P = k\Delta l, \quad (1)$$

and therefore, the elastic energy accumulated in the part will be:

$$U_E = \frac{P\Delta l}{2} = \frac{P^2}{2k}. \quad (2)$$

If crack growth ($a + \Delta a$) occurs under the load P , the stiffness k of the part will also decrease to the k' as seen in Fig. 2.

The strain energy released rate as a result of the change in stiffness with increasing crack length is given by Eq. (3):

$$G_I = -\frac{1}{2} P^2 \frac{d(1/k)}{da}, \quad (3)$$

The equivalent of the strain energy released rate G_I in case of a unit progression of the crack in Eq. (3) can also be expressed in a different way in Eq. (4):

$$G_I = \frac{1}{2} P^2 \frac{d(1/k)}{da} = \frac{\pi a \sigma^2}{E}. \quad (4)$$

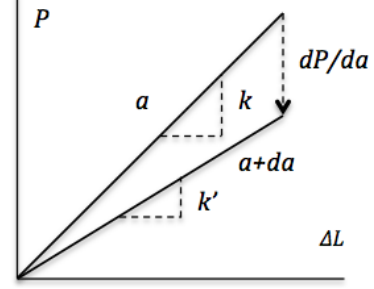


Fig. 2 Displ. controlled load-displacement schematic plot

In Eq. (4) a is the crack length; σ is the applied stress; Y is the geometric correction factor; E is the modulus of elasticity; W denotes the specimen width. Let the thickness value be expressed by B . If σWB is written instead of the load P for the tensile sample in the equation and the compliance of the linear part L/EWB in the load-displacement plot of the unnotched specimen $a = 0$ is written for the integral constant, the equivalent of the stiffness in Eq. (5) is reached:

$$k = \frac{E_{11}}{\frac{1}{B} \left[\pi (a/W)^2 Y^2 + \frac{L}{W} \right]}. \quad (5)$$

Eq. (5) is not only valid for obtaining the modulus of elasticity from the load-displacement plot of the cracked specimen, but also provides the stiffness k value at each relative crack length ratio a/W if the modulus is only known parameter. The Y , the geometric correction factor, shall have the values in Table 1 for the clamped-end tensile specimen. The factor for the pin-loaded tensile specimen is given in the relevant reference [23].

Table 1

The geometric corr. factors Y for the clamped-end single side-cracked tensile specimen [24]

a/W	Blatt et al.	Marchand et al. and Ahmed et al.	Dao and Mettu	Bowie et al.
0.05	1.1227	1.14	1.1389	1.13
0.1	1.1528	1.166	1.1581	1.16
0.2	1.2411	1.251	1.2291	1.25
0.3	1.3654	1.378	1.3604	1.37
0.4	1.5147	1.539	1.5178	1.52
0.5	1.6951	1.726	1.7029	1.7
0.6	1.9026	1.934	1.9192	1.91
0.7	2.1569	2.171	2.1801	2.17
0.8	2.498	2.481	2.5322	
0.9	3.1502	3.113	3.1637	
0.95	4.0864	4.052	4.137	

Consider the situation in which the crack propagates in a controlled manner due to stress in a laminated composite material with a fibre structure in the load direction. The crack will deviate from its axis and progress at the fiber-matrix interfaces. The damage in front of the crack tip will lead to fiber fractures due to the increased stress. In particular, fiber breaks will bring along oscillations (zig-zag characteristic) in the $P - \Delta l$ graph and will gradually reduce the stiffness of the material. Therefore, the ratio of the

applied load and the corresponding displacement measured during a mechanical test will give the instant stiffness. Using this instant value in Eq. (5) will give the instant crack length equivalent.

In order to determine the instantaneous crack lengths in Eq. 5, the expression $(a/W)Y$ should be known, as in Eq. (6):

$$(a/W)Y = \left[\frac{1}{\pi} \left(\frac{E_{11}B}{k} - \frac{L}{W} \right) \right]^{1/2}. \quad (6)$$

Since the geometric correction factor Y is the polynomial expression of a/W , the function of the graph $(a/W)Y$ will make the transition from $(a/W)Y$ to crack length ratio a/W and then to crack length a .

Although the crack is a branched state in the laminated composite materials, this state has an effective counterpart (Fig. 3). The crack length just mentioned is the effective response of the propagation. The treatment of the effective crack length with its corresponding stress will give the critical fracture toughness. The R -curve of the material can also be reached from the critical fracture toughness.

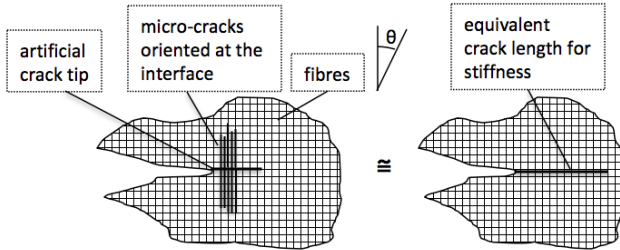


Fig. 3 Schematic view of equivalent crack length of laminated composite material for stiffness

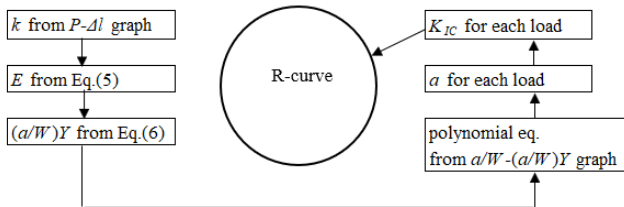


Fig. 4 The process flow chart of the specified method

3. Material and method

The $[0/90]_{4s}$ single edge-cracked non-crimped E-glass/epoxy composite laminate tensile specimen was used for the methodology. The test specimen was cut to size with a diamond cutter (Fig. 5).

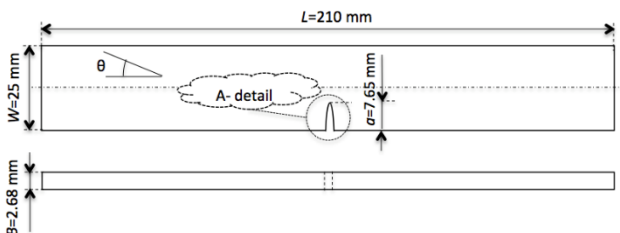


Fig. 5 Dimension of test specimen

An artificial notch was formed on one edge of the specimen using a diamond cutter bit. A (diamond) dremel

bit with a thickness of 0.45 mm and a depth of 1.0 mm was used for artificial crack formation at the notch tip (Fig. 6).

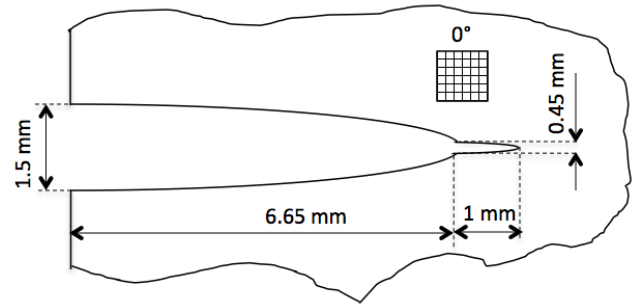


Fig. 6 Dimension of the artificial crack (A-detail of Fig. 5)

The length, the width and the thickness of the specimen are 210 mm, 25 mm and 2.68 mm, respectively. The crack length to width ratio a/W is 0.306 and the specimen is shown as the Example-1 in Fig. 4. The extensometer distance (L in Eq. 5 and 6) was 56.18 mm as a reference. The fibre volume ratio is 45%. The ambient temperature of the test performed at a speed of 5 mm/min is 22°C and the relative humidity is 35%.

4. Results

While the a/W ratio of two of the four specimens from the same structure and material given in Fig. 7 is at the levels of 0.2, the a/W ratios of the other two are at the levels of 0.3.

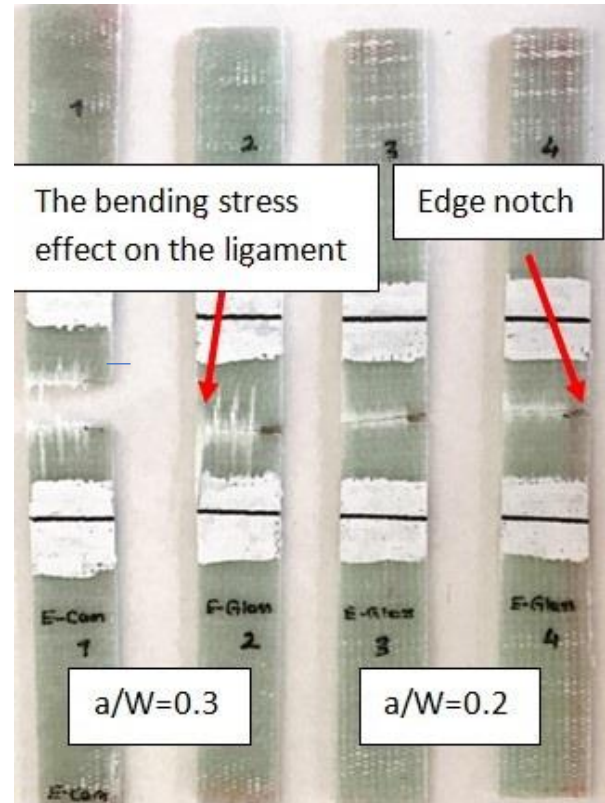


Fig. 7 The E-glass/epoxy SENT specimens after tensile testing

It will be important to note that during controlled crack propagation, in the specimens with $a/W = 0.3$ ratio, a compressive force occurs at the opposite edge and separates the outer longitudinal fibers from the matrix, but this is not

observed in specimens with $a/W = 0.2$ ratio, and the fibres were cut planely in the crack path.

Therefore, it should be noted that the selected crack length ratio may also have an effect on the R -curve.

It is seen in Fig. 8 that the maximum load at the level of 7465 N corresponds to an elongation of 0.477 mm. The slope of the linear part of the curve (stiffness) is obtained as 21339 N/mm. If values are entered in Eq. (5), the elasticity modulus E_{11} for $a/W = 0.306$ is determined at the level of 22 GPa.

In Table 2, the 6 of the 505 data obtained from the $P - \Delta l$ graph are given.

The polynomial equation obtained from the $a/W - (a/W)Y$ graph (Fig. 9) was used to reach the a/W crack length ratio from the $(a/W)Y$ in Table 2. The factors of Table 1 were used since the tensile test was performed under the clamped-end condition in which moment transfer was partially restricted.

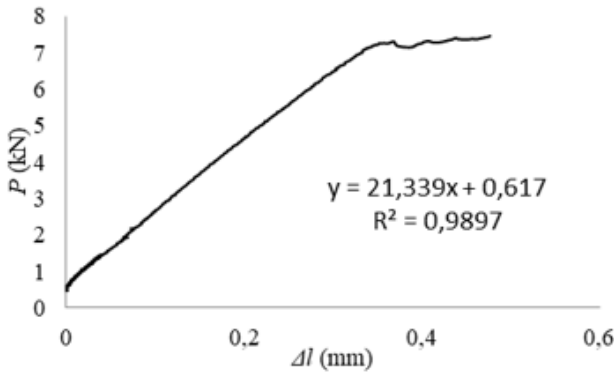


Fig. 8 E-glass/epoxy load-displacement graph

Table 2

Obtaining E-glass/epoxy sample data according to Fig. 3

P, N	$\Delta l, mm$	$k, N/mm$	$(a/W)Y$	a, mm	$G_{IC}, N/mm$
4278	0.181	20 873	0.433	7.64	8.45
5006	0.218	20 635	0.445	7.80	11.93
5715	0.257	20 265	0.463	8.05	16.27
6475	0.299	19 966	0.478	8.23	21.64
7200	0.346	19 342	0.509	8.62	28.70
7465	0.477	14 590	0.759	11.08	48.05

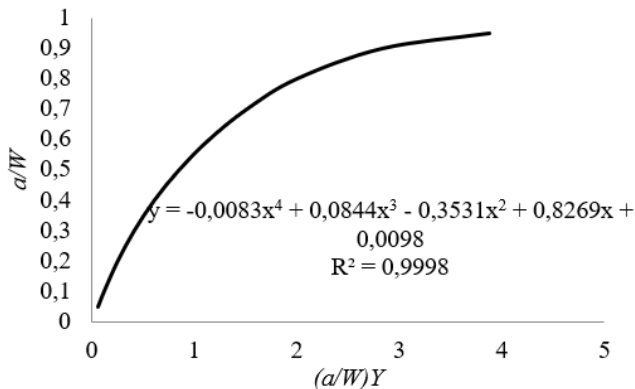


Fig. 9 The $a/W - (a/W)Y$ graph prepared from Table 1

Using Fig. 9, the crack length a is obtained from the crack length ratio a/W corresponding to each load value. In Table 2, it is seen that the initial crack length of 7.65 mm reaches 11.08 mm. The Δa (3.43 mm) is the effective crack length and shows the total amount of propagation of the crack that has branched and propagated in its own direction.

At the end of the controlled crack progression, strain energy release rate G_{IC} reaches 48.05 N/mm as seen in the last column of Table 2.

The $P - \Delta l$ curve of the specimen shows that the maximum load is 7466 N as seen in Fig. 8. This corresponds to a critical fracture stress σ_r of 111.4 MPa. The crack propagation of the $P - \Delta l$ graph, part of which is given in Table 2, is used but the maximum stress of 111.4 MPa is fixed in the Eq. (7), the G -curve will be formed. Of course, the geometrical factor Y in Eq. (7) will obtain its value depending on the varying crack length a .

$$G_{IC} = \frac{\sigma^2 Y^2 \pi a}{E}. \quad (7)$$

Fig. 10 is the R -curve (fracture energy-crack length plot) obtained from the $P - \Delta l$ plot. In the graph created by using all (505) data, it is seen that a zig-zag curve is formed up to 8.45 mm and 27 N/mm. Beyond this point, the curve has a flatter structure. This may be related to the propagation of the crack branching from the crack tip and consequent fiber breaks. Beyond 8.45 mm, damage area around the crack tip and increased stress may have triggered a more planar propagation of the crack.

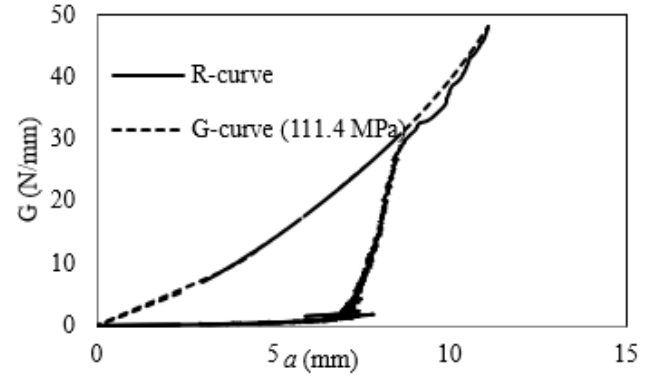


Fig. 10 The driving G and the resistive R -curves

In planar progression, compressive stress acting on the opposite edge of the specimen is also likely to have an effect on the characteristic of the curve. In the first place, the specimen will try to resist the compressive force. However, with the propagation of the controlled crack, the effect of the pressure on the opposite edge will increase and the bending moment will be more pronounced in the specimen under tensile stress. This will create a factor that facilitates the opening of the crack tip. This will be another factor that ensures the planar propagation of the crack. Fig. 10 shows that the methodology outlined in this study is appropriate in terms of reflecting the fracture detail unique to composite materials.

The fracture toughness obtained at the end of controlled crack propagation is expressed as critical fracture toughness. The R and G -curves are tangent at this point and the R -curve shows this fracture toughness K_{IC} . Another fracture toughness as important as this one is to determine the value at which the crack starts to propagate. The fracture toughness encountered at the crack length corresponding to the 2% increment $[(\Delta a/a)100]$ is the initial fracture toughness and is expressed as the candidate fracture toughness K_Q . This also describes the point where the line drawn by reducing the slope of the linear part of the load-displacement

curve by 5 % intersects the curve [17, 25]. In this study, the controlled crack propagation amount Δa of the specimen with an initial crack length of 7.65 mm is 3.43 mm. According to the standard, the value at $a = 7.8$ mm is the candidate fracture toughness. According to process stated in Fig. 4 and Table 2, the candidate fracture toughness corresponding to 7.8 mm is determined as 513 MPa.mm^{1/2}.

5. Model verification

The amount of opening at the crack mouth in a single-sided crack tensile specimen is expressed by Eq. (8) [23]:

$$CMOD = \frac{4\sigma a}{E} \left[\frac{1.46 + 3.42 \left(1 - \cos \frac{\pi a}{2W} \right)}{\left(\cos \frac{\pi a}{2W} \right)^2} \right]. \quad (8)$$

When the crack propagation determined for each load using the specified method in this paper is placed in Eq. (8), it can be seen from Fig. 11 that the CMOD values obtained and the extensometer elongation are almost equal.

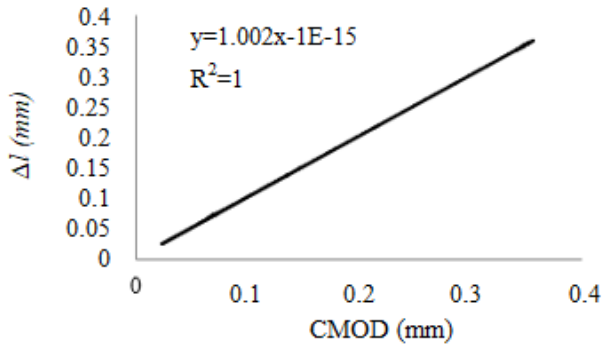


Fig. 11 The stiffness (extens.) - CMOD plot

The general expression for the CTOD for the plane stress condition is given in Eq. (9) [26]:

$$CTOD = \frac{K_{IC}^2}{E\sigma_0}. \quad (9)$$

Eq. (10) is reached if the equation above is arranged to give the critical fracture stress:

$$\frac{\sigma_r}{\sigma_0} = \frac{(CTOD)E}{K_{IC}^2 Y (\pi a)^{1/2}}. \quad (10)$$

The ratio of the critical fracture stress σ_r to the tensile strength σ_0 for the single edge-cracked tensile specimen is approximately found with the help of Eq. (11) or (12). The difference between Eqs. (11) and (12) is due to the geometric correction factor Y . If the factors in Table 1 are used, Eq. (11) should be used, if the polynomial equation in reference [23] is used, Eq. (12) should be used.

$$\frac{\sigma_r}{\sigma_0} = \frac{1.059}{Y} \left[\frac{1.2732}{a} \right]^{1/2}, \quad (11)$$

$$\frac{\sigma_r}{\sigma_0} = \left[\frac{1.2732}{Ya} \right]^{1/2}. \quad (12)$$

If Eq. (11) is adapted to Eq. (9), a different expression of the CTOD is achieved as seen in Eq. (13). Eq. (13) shows that the value of CTOD changes only with the stress intensity factor (SIF) occurred at each crack increment.

$$CTOD = 2.118 \frac{K_{IC}}{E}. \quad (13)$$

So, it can be predicted that the approach proposed in this paper will yield results consistent with the $P - CMOD$ curve, excluding composite materials that have the crack formation outside the crack zone under stress, such as polyester matrix.

Fig. 12 shows the function between the Δl in the length of the extensometer and the CTOD. Except for the region close to the maximum load, it can be stated that the linear characteristic is present.

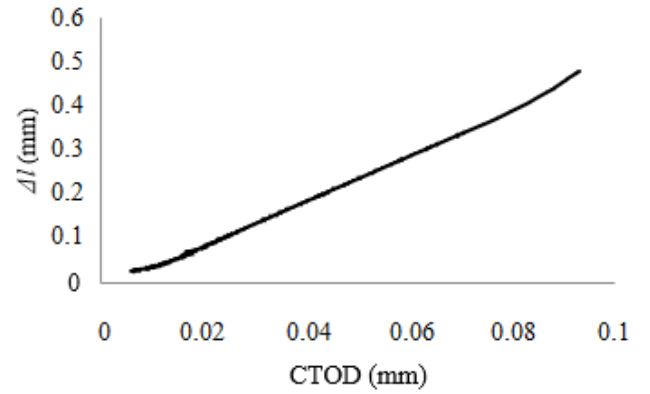


Fig. 12 The stiffness (extens.)-CTOD (from Eq. (13)) plot

In a study, the effects of dimensional parameters such as specimen thickness and aspect ratio on fracture toughness were investigated on a short fibre glass composite [10]. The compliance values in the linear portion of the $P - CMOD$ plot is normalized by multiplying the modulus of elasticity E and the corresponding thickness B . It was stated that the closest result to the actual values was obtained in the range of $a/W = 0.3 - 0.5$. It may be noted that this normalization comes from Eq. (5) established in this paper.

6. Conclusions

In this study, the displacement values obtained by the extensometer, which is an easier approach, were used to construct the R -curve instead of the CTOD. Undoubtedly, CTOD will give much more precise results, as it addresses the crack tip. However, it can be stated that the method proposed in this study will give positive results in terms of ease of application and the continuity of the R -curve. Since the specified method is based on Linear Elastic Fracture Mechanics, it will give more accurate results for materials with linear elastic characteristics.

References

1. Chakraborty, D.; Murthy, K.; Chakraborty, D. 2017. Experimental determination of mode I stress intensity

- factor in orthotropic materials using a single strain gage, *Engineering Fracture Mechanics* 173: 130-145.
<https://doi.org/10.1016/J.ENGFRAC-MECH.2017.01.002>.
2. **Toygari, M. E.; Toparli, M. B.; Uyulgan, B.** 2006. An Investigation of fracture toughness of carbon/epoxy composites, *Journal of Reinforced Plastics and Composites* 25: 1887 - 1895.
<https://doi.org/10.1177/0731684406069916>.
 3. **Kolednik, O.; Predan, J.** 2022. Influence of the material inhomogeneity effect on the crack growth behavior in fiber and particle reinforced composites, *Engineering Fracture Mechanics*.
<https://doi.org/10.1016/j.engfracmech.2021.108206>.
 4. **Fu, S.; Lauke, B.; Mai, Y.** 2009. *10-Fracture mechanics. Science and Engineering of Short Fibre Reinforced Polymer Composites*. Woodhead Publishing, 1st Edition.
<https://doi.org/10.1533/9781845696498.231>.
 5. **Gaggari, S. K.; Broutman, L. J.** 1975. Crack growth resistance of random fiber composites, *Journal of Composite Materials* 9: 216 - 227.
<https://doi.org/10.1177/002199837500900301>.
 6. **Zhu, X. K.; Leis, B. N.** 2008. Experimental determination of J-R curves using SENB specimens and P-CMOD Data, ASME Paper No. PVP2008- 61219.
<https://doi.org/10.1115/PVP2008-61219>.
 7. **Camanho, P. P.; Ercin, G. H.; Catalanotti, G.; Mahdi, S.; Linde, P.** 2012. A finite fracture mechanics model for the prediction of the open-hole strength of composite laminates, *Compos Part A Appl. Sci. i Manuf.* 43(8): 1219-1225.
<https://doi.org/10.1016/J.COMPOSITESA.2012.03.004>.
 8. **Ercin, G. H.; Camanho, P. P.; Xavier, J.; Catalanotti, G.; Mahdi, S.; Linde, P.** 2013. Size effects on the tensile and compressive failure of notched composite laminates, *Compos. Struct.* 96(0): 736-744.
<https://doi.org/10.1016/J.COMPSTRUCT.2012.10.004>.
 9. **Martin, E.; Leguillon, D.; Carrere, N.** 2012. A coupled strength and toughness criterion for the prediction of the open hole tensile strength of a composite plate, *Int J. Solids Struct.* 49(26): 3915-3922.
<https://doi.org/10.1016/J.IJSOLSTR.2012.08.020>.
 10. **Catalanotti, G.; Camanho, P. P.** 2013. A semi-analytical method to predict net-tension failure of mechanically fastened joints in composite laminates, *Compos. Sci. Technol.* 76(0): 69-76.
<https://doi.org/10.1016/J.COMPOSITECH.2012.12.009>.
 11. **Catalanotti, G.; Arteiro, A.; Hayati, M.; Camanho, P. P.** 2014. Determination of the mode I crack resistance curve of polymer composites using the size-effect law, *Engineering Fracture Mechanics* 118: 49-65.
<https://doi.org/10.1016/J.ENGFRAC-MECH.2013.10.021>.
 12. **Kuhn, P.; Catalanotti, G.; Xavier, J.; Ploeckl, M.; Koerber, H.** 2018. Determination of the crack resistance curve for intralaminar fiber tensile failure mode in polymer composites under high rate loading, *Composite Structures*.
<https://doi.org/10.1016/J.COMPSTRUCT.2018.07.039>.
 13. **Agarwal, B. D.; Giare, G. S.** 1981. Crack growth resistance of short fibre composites: I-Influence of fibre concentration, specimen thickness and width, *Fibre Science and Technology* 15: 283-298.
[https://doi.org/10.1016/0015-0568\(81\)90053-1](https://doi.org/10.1016/0015-0568(81)90053-1).
 14. **Kumar, A.; Pandey, R. K.; Nanda, A.** 1987. Crack growth characterization in a short fibre glass-epoxy composite, *Composites Science and Technology* 29: 17-32.
[https://doi.org/10.1016/0266-3538\(87\)90034-0](https://doi.org/10.1016/0266-3538(87)90034-0).
 15. **Morris, D. H.; Hahn, H. T.** 1977. *Fracture Resistance Characterization of Graphite/Epoxy Composites*, ASTM special technical publications, p. 5-17.
<https://doi.org/10.1520/STP26932S>.
 16. **Wells, J. K.; Beaumont, P. W.** 1987. The prediction of R-curves and notched tensile strength for composite laminates, *Journal of Materials Science* 22: 1457-1468.
<https://doi.org/10.1007/BF01233148>.
 17. **Garg, A. C.; Trotman, C. K.** 1980. Influence of water on fracture behaviour of random fiber glass composites, *Engineering Fracture Mechanics* 13: 357-370.
[https://doi.org/10.1016/0013-7944\(80\)90065-X](https://doi.org/10.1016/0013-7944(80)90065-X).
 18. **Mojtahed, M.; Zachary, L. W.** 1987. Use of photoelasticity to determine orthotropic K_I stress-intensity factor, *Exp. Mech.* 27: 184-9.
<https://doi.org/10.1007/BF02319472>.
 19. **Baik, M. C.; Choi, S. H.; Hawong, J. S.; Kwon, J. D.** 1995. Determination of stress intensity factors by the method of caustics in anisotropic materials, *Exp. Mech.* 35: 137-43.
[https://doi.org/10.1016/S0266-3538\(02\)00154-9](https://doi.org/10.1016/S0266-3538(02)00154-9).
 20. **Yao, X.; Chen, J.; Jin, G.; Arakawa, K.; Takahashi, K.** 2004. Caustic analysis of stress singularities in orthotropic composite materials with mode-I crack, *Compos Sci. Technol.* 64: 917-24.
[https://doi.org/10.1016/S0266-3538\(02\)00154-9](https://doi.org/10.1016/S0266-3538(02)00154-9).
 21. **Mogadpalli, G. P.; Parameswaran, V.** 2008. Determination of stress intensity factor for cracks in orthotropic composite materials using digital image correlation, *Strain* 44: 446-52.
<https://doi.org/10.1111/j.1475-1305.2007.00391.x>.
 22. **Agarwal, B. D.; Patro, B.; Kumar, P.** 1985. Crack length estimation procedure for short fiber composites: An experimental evaluation, *Polymer Composites* 6: 185-190.
<https://doi.org/10.1002/pc.750060311>.
 23. **Tada, H.; Paris, P. C.; Irwin, G. R.** 2000. *The Stress Analysis of Cracks Handbook*, Third Edition. ASME Press, New York.
<https://doi.org/10.1115/1.801535>.
 24. **Blatt, D.; John, R.; Coker, D.** 1994. Stress intensity factor and compliance solutions for a single edge notched specimen with clamped ends, *Engineering Fracture Mechanics* 47: 521-532.
[https://doi.org/10.1016/0013-7944\(94\)90252-6](https://doi.org/10.1016/0013-7944(94)90252-6).
 25. ASTM E 1820-01. 2003. *Standard Test Method for Measurement of Fracture Toughness*, ASTM International, West Conshohocken, PA.
 26. **Srivastava, V. K.** 1990. Measurement of fracture strength of notched thick composites on the use of CTOD, *Engineering Fracture Mechanics* 36: 137-144.
[https://doi.org/10.1016/0013-7944\(90\)90103-N](https://doi.org/10.1016/0013-7944(90)90103-N).

G. Saracoglu

OBTAINING THE FRACTURE RESISTANCE CURVE USING THE GENERAL DISPLACEMENT

S u m m a r y

In this paper, the energy release energy corresponding to the unit crack propagation obtained from the displacement-controlled load-displacement plot is equalized to the elastic energy release rate, and the variation of stiffness based on the crack length is obtained. For this purpose,

instead of measuring the amount of crack mouth opening in the single edge-cracked tensile specimen, the extensometer elongation amount was taken in the middle part of the specimen. Thanks to the equality of the stiffness to the crack length, the transformation of the load-displacement curve into the material resistance curve was realized.

Keywords: resistance curve; strain energy release rate; load-displacement curve; fracture toughness.

Received May 09, 2022

Accepted January 27, 2023



This article is an Open Access article distributed under the terms and conditions of the Creative Commons Attribution 4.0 (CC BY 4.0) License (<http://creativecommons.org/licenses/by/4.0/>).